N-Aminoporphyrins. Preparation and Metal Complexes. Structure of *N*-Tosylamino-5,10,15,20-tetraphenylporphinatonickel(II)

H. J. Callot,*[1a] B. Chevrier,[1b] and R. Weiss*[1b]

Contribution from the Institut de Chimie, Université Louis Pasteur, 67000 Strasbourg, France. *Received January 13, 1978*

Abstract: The reaction between azides and porphyrins or Zn porphyrins gave either azahomoporphyrins or *N*-aminoporphyrins depending on the reagent. *N*-Tosyl and *N*-*p*-nitrobenzoylamino-5,10,15,20-tetraphenylporphins gave neutral complexes on reaction with divalent cations like Ni(II), Cu(II), and Zn(II). These complexes correspond to the insertion of a nitrene moiety into a metal–N bond of a metalloporphyrin. The precise structure of *N*-tosylamino-5,10,15,20-tetraphenylporphinatonickel-(II) has been determined by x-ray diffraction. Crystals were obtained as the CH_2Cl_2 solvate from CH_2Cl_2/CH_3OH solutions. The space group is $P\bar{1}$. The triclinic unit cell contains two molecules and has $a = 14.378$ (7), $b = 14.002$ (7), $c = 11.750$ (5) Å and $\alpha = 95.62$ (8), $\beta = 102.98$ (8), $\gamma = 102.19$ (8)°. The structure was anisotropically refined to $R_1 = 0.061$ and $R_2 = 0.087$ for the 4413 unique reflections having $I > 3\sigma_I$. The nickel is tetracoordinated with nitrogen atoms of only three pyrrole bases and with the extra nitrogen atom of the nitrene fragment. The four pyrrole nitrogens are approximately coplanar. The nickel atom lies out of the four nitrogen mean plane (4N) by 0.21 Å and the extra nitrogen lies by 0.94 Å on the same side as the nickel. The porphyrin macrocycle is distorted. The distortion is such that the pyrrole ring affected by the nitrene insertion exhibits a very large angle of 40.5° with the (4N) plane, the other pyrroles making smaller angles of 1.8, 4.4, and 9.4°.

The homologation of the porphyrinic macrocycle can be achieved by the reaction of metalloporphyrins with diazo esters[2] or the reaction of a free base with a nitrene,[3] to yield homo- and azahomoporphyrins such as **1** and **2.**

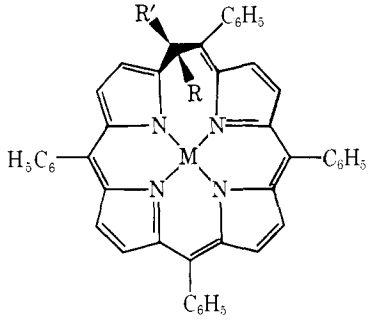

1

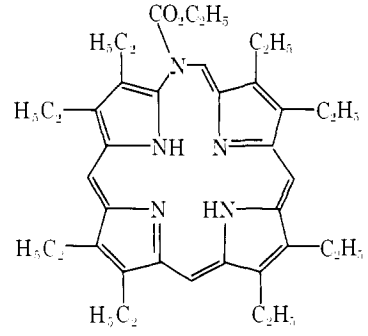

2

The stability of the type **1** compounds (TPP series), as compared to that of analogous octaalkyl derivatives, allowed us to infer that azahomoporphyrins (TPP series) should be more stable and thus easier to study than compound **2,** whose thermal ring contraction to *meso*-aminoporphyrin occurred easily.

In a recent paper,[4] Ichimura described a photochemical meso amination of zinc octaethylporphin (ZnOEP) using azides. Since an azahomoporphyrin is a likely intermediate in this reaction we submitted ZnTPP **3** to Ichimura's conditions. In the present paper we report that the reaction took an unexpected course and provided a route to a series of *N*-aminoporphyrins, aza analogues of the known *N*-alkylporphyrins,[5] while using a different nitrene precursor leads to azahomoporphyrins.

Results

A simplified procedure was used, compared to that of Ichimura: (a) sunlight is efficient enough to promote the reaction; (b) oxygen quenching proved to be low, at least when tosyl and *p*-nitrobenzoyl azides were used.

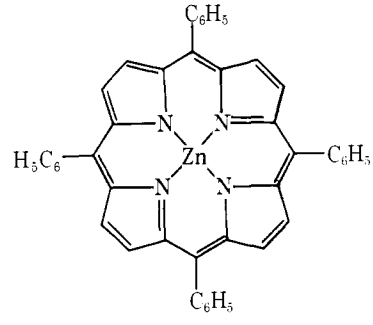

3

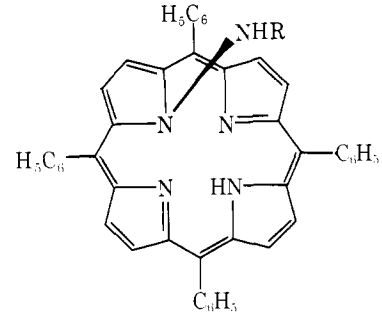

4, R = $CH_3C_6H_4SO_2$
5, R = $O_2NC_6H_4CO$

The resulting zinc complexes were found to be unstable toward chromatographic treatment and thus were demetalated to the free bases **4** and **5** prior to the purification step. The spectral data of **4** and **5** are typical for N-substituted porphyrins: (a) shift of the visible absorption toward longer wavelength compared to normal porphyrins; (b) strong shielding (NMR) of the aromatic protons of the tosyl and *p*-nitrobenzoyl groups (of the order of 3–4.5 and 1–2 ppm for ortho and meta

0002-7863/78/1500-4733$01.00/0

protons); (c) characteristic shielding of the pyrrolic protons of the modified ring (ca. 1 ppm).

Modifications of the reaction substrate and conditions gave the following results: (a) In the absence of Zn the free base did not react photochemically with RN_3. (b) Thermal reaction (ZnTPP + TsN_3) required drastic conditions (140 °C, 24 h) and led to a complex mixture that did not contain product **4**. (c) Catalysis by copper powder promoted a different reaction pathway leading to sulfone **6** in low yield (no **4** could be detected).

Sulfone **6** was also characterized as its nickel(II) complex **7**. Polarographic measurements[6] added evidence for structure **7**, since the observed first reduction wave was displaced by 0.2 V toward less negative potentials compared to H_2TPP as expected in the presence of a strong electron-withdrawing substituent.[7]

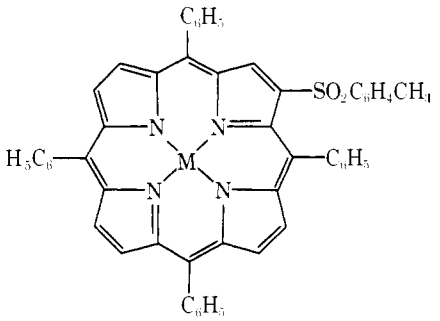

6, M = H_2
7, M = Ni

Attempts to use different nitrene precursors led to various results: (a) Reaction with N_3COOR (R = alkyl, benzyl) gave only polar mixtures while on degassing almost no reaction occurred (only traces of products were observed and could not be isolated). (b) Reaction of the free base H_2TPP with *p*-$NO_2C_6H_4SO_3NHCO_2Et$[8] gave a complex mixture in which no *N*-aminoporphyrin was present but instead compounds **8** and **9**.

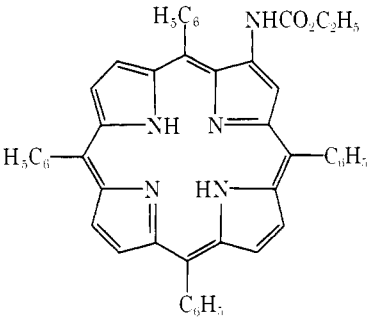

8

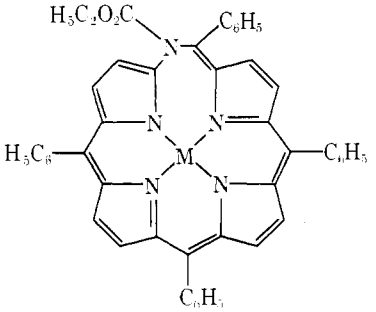

9, M = H_2
10, M = Ni

While **8** was easily identified as a "normal" porphyrin, **9** and its nickel(II) complex **10** showed spectral data similar to that of the known homoporphyrins.[2] The stability of **9** (unchanged in refluxing toluene) was larger than that of **2** (ring contraction in refluxing chloroform). Complex **10** was stable in the solid state and at 25 °C in CH_2Cl_2 solution, although it decomposed to a complex mixture in the presence of methanol.

Metalation of **4** and **5** gave complexes **11–15.** All are neutral compounds of low polarity (TLC). Unambiguous proof for the proposed skeleton was established by x-ray diffraction (see below).

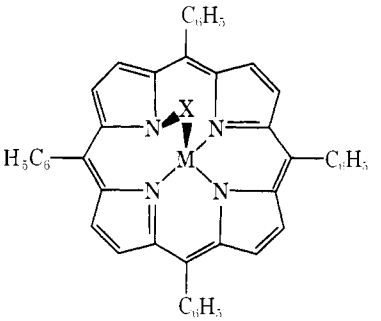

11, X = $NSO_2C_6H_4CH_3$; M = Ni
12, X = $NSO_2C_6H_4CH_3$; M = Cu
13, X = $NSO_2C_6H_4CH_3$; M = Zn
14, X = $NCOC_6H_4NO_2$; M = Ni
15, X = $NCOC_6H_4NO_2$; M = Cu

Compounds **11–15** showed data similar to that of **19** (see below): (a) visible spectra of the "normal" metalloporphyrin type, (b) large shielding (NMR) of the R group. As expected complexes **11, 12, 14,** and **15** (M = Ni, Cu) showed very similar visible data, whereas band positions for **13** (M = Zn) are shifted toward greater wavelengths.

Metalation by Co(II) seemed, according to the initial coloration, to give an analogous derivative, although its instability prevented isolation.

Metalation of **4** by Hg(II) (as $HgCl_2$ in the presence of a base) gave a different type of product of composition: base + $2HgCl_2$ − 2HCl. From its "base-like" (Soret + four peaks) visible data and NMR ^{199}Hg–^1H coupling constants we tentatively assigned structure **16.** (The red shift of the maximum

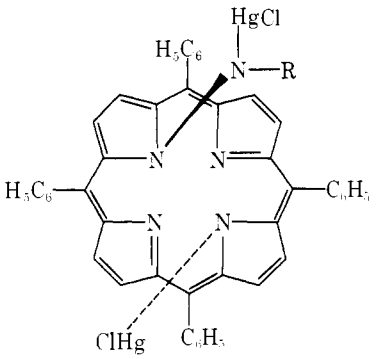

16

was consistent with the distortion of the porphyrin ring that would be found in structure **16.**) Such a structure is similar to that proposed for the *N*-methylOEP–HgOAc product previously isolated by Smith.[9] The NMR data of **16** showed three different types of ^{199}Hg–^1H coupling constants: small (5.8 Hz) for the pyrrolic protons of the *N*-amino-substituted ring, small again (ca. 5.5–6.0 Hz) for the protons of the unsubstituted pyrrole rings, and larger (21.0 Hz) for the N–Hg-substituted ring.

Discussion

The various reactions involving porphyrins or metalloporphyrins and nitrene precursors illustrate four different reaction pathways, namely, N-amination, macrocycle homologation, and acylamino or tosyl insertion in a pyrrolic C–H bond.

The observed photochemical reaction is most probably, as in Ichimura's conditions, initiated by the known transfer of triplet energy from ZnTPP to the reagent.[10] The lack of oxygen quenching proves that the observed pathway competed efficiently with those involving O_2. Although polar photooxidation products could be detected, their yield remained at a negligible level.[11]

The regiospecificity of the photochemical reaction showed the most dramatic effect since the amination site was shifted from a bridge double bond (if one assumes an intermediate aziridine) to a pyrrolic nitrogen on changing from OEP series to TPP series. An interpretation of our results may involve both a steric hindrance and a decrease of reactivity of the meso positions due to the introduction of the phenyl substituents. However, one must also remember that the thermally generated carboethoxynitrene did not show the same change of reaction site but formed an azahomoporphyrin as it did in the OEP series.[3]

Again an explanation is to be found for the formation of two types of insertion products. Occurrence of **8** was expected since such an insertion in an aromatic C-H bond is well documented.[12] On the other hand, to our knowledge, no sulfone was formed on reaction of sulfonylazides with aromatics.[13]

Comparison of the above reactions with those initiated by carbene (or carbenoid) precursors like diazoalkanes[2,14] shows similarities. In both cases all three major reaction pathways are present: (a) functionalization of a pyrrolic nitrogen, (b) ring enlargement at the meso position, (c) modification of the pyrrole ring to give either fused cyclopropanes or aminoporphyrins.

The insertion of a divalent metal ion into the *N*-aminoporphyrin ligand could formally give two different types of complexes: (a) cationic or halogen-containing derivatives through bond formation between the metal and the four pyrrolic nitrogens, as was shown for most *N*-alkylporphyrins,[15] (b) bonding of three pyrrolic nitrogens and formation of a metal-supplementary nitrogen bond; this should give a neutral complex.

It is noteworthy that in one case,[16] a carbon analogue **17** of *N*-aminoporphyrins formed neutral complex **19** via cationic **18.** The precise structure of **19** has been determined by x-ray diffraction.[16,17] Except for the case of mercury(II) all divalent cations gave neutral products, aza analogues of **19.** All **11–15** showed spectral data similar to that of **19.** The precise structure of the mercury compound is still to be determined. However a "sitting-atop" complex like structure **16** agrees with (a) the measured ^{199}Hg-^{1}H coupling constants, (b) the known tendency for mercury to form rather stable intermediates during the metallation of porphyrins,[9,18] (c) the known mercury(II) derivatives of tosylamides.[19]

Structure of Compound 11. Figure 1 is a computer-drawn model[20] of the molecule as it exists in the crystal. Also displayed in Figure 1 are the special symbols used to identify the atoms. Individual bond lengths and angles are given in Tables I and II. In this compound, the *N*-tosyl moiety appears as inserted into a Ni-N bond of the nickel(II) *meso*-tetraphenylporphin. The nickel atom is then tetracoordinated with the extra nitrogen atom N5 and with the pyrrole nitrogen atoms N2, N3, and N4. The pyrrole nitrogen N1 is not bonded to the nickel as shown by the large Ni···N distance of 2.639 (4) Å. The Ni-N3 bond trans to the N5 position is somewhat shorter than the other two Ni-N distances (1.883 (4) Å for Ni-N3 vs. 1.920 (4) Å for the two equivalent Ni-N2 and Ni-N4 distances). The shortest Ni-N5 bond length of 1.830 (4) Å is close to that observed in diamagnetic square planar nickel complexes.[21]

The four pyrrole nitrogens are approximately coplanar (Table III). The nickel lies out of the four nitrogen mean plane by 0.21 Å. The extra nitrogen N5 is considerably removed from

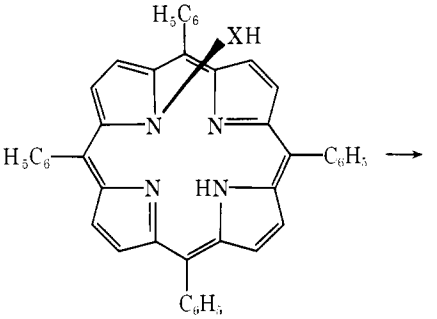

17, X = $CHCO_2C_2H_5$
(**4**, **5**, X = NR)

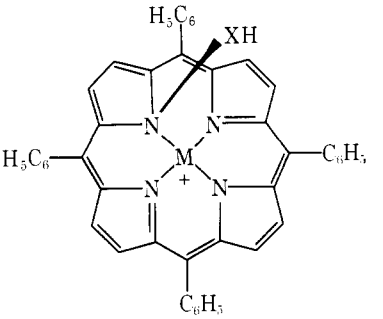

18, X = $CHCO_2C_2H_5$;
M = Ni

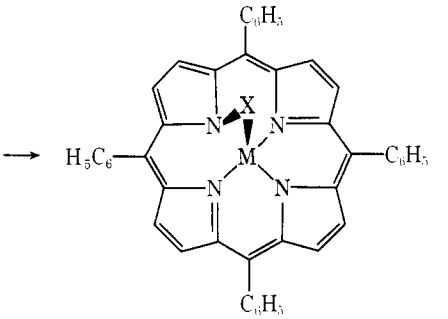

19, X = $CHCO_2C_2H_5$;
M = Ni
(**11–15**, X = NR;
M = Ni, Cu, Zn)

the (4N) plane; its displacement of 0.94 Å is in the same direction as that of the nickel atom but opposite to that of nitrogen N1. Mean planes were determined by the method of least squares[22] (Table III).

Whereas in classical porphinato complexes the pyrrole rings are nearly coplanar with the (4N) plane, the porphyrin macrocycle is here distorted. Thus individually planar pyrrole rings (N1) to (N4) make dihedral angles of 40.5, 1.8, 4.4, and 9.4° with the (4N) plane. The porphine skeleton departures from a planar configuration are also indicated in Figure 2. The distortion is such that the pyrrole ring (N1) is rotated toward the nickel atom while the other three pyrroles remain approximately coplanar with the (4N) plane. The present distortion can be closely compared with that recently described[16,17] for compound **19,** but differs from that observed for *N*-alkylporphyrin metal complexes in which the pyrrole ring (N1) is rotated in the reverse direction with respect to the metal.[15b]

Using C_a and C_b to denote the respective α- and β-carbon atoms of a pyrrole ring, C_m for methine carbon, and C_p for a phenyl carbon atom that is bonded to the core, the averaged bond lengths in the porphine skeleton are N-C_a = 1.382 (7), C_a-C_b = 1.437 (9), C_b-C_b = 1.340 (8), Ca-C_m = 1.397 (8), and C_m-C_p = 1.489 (7) Å, wherein the number in parentheses is the greatest value of the estimated standard deviation for an

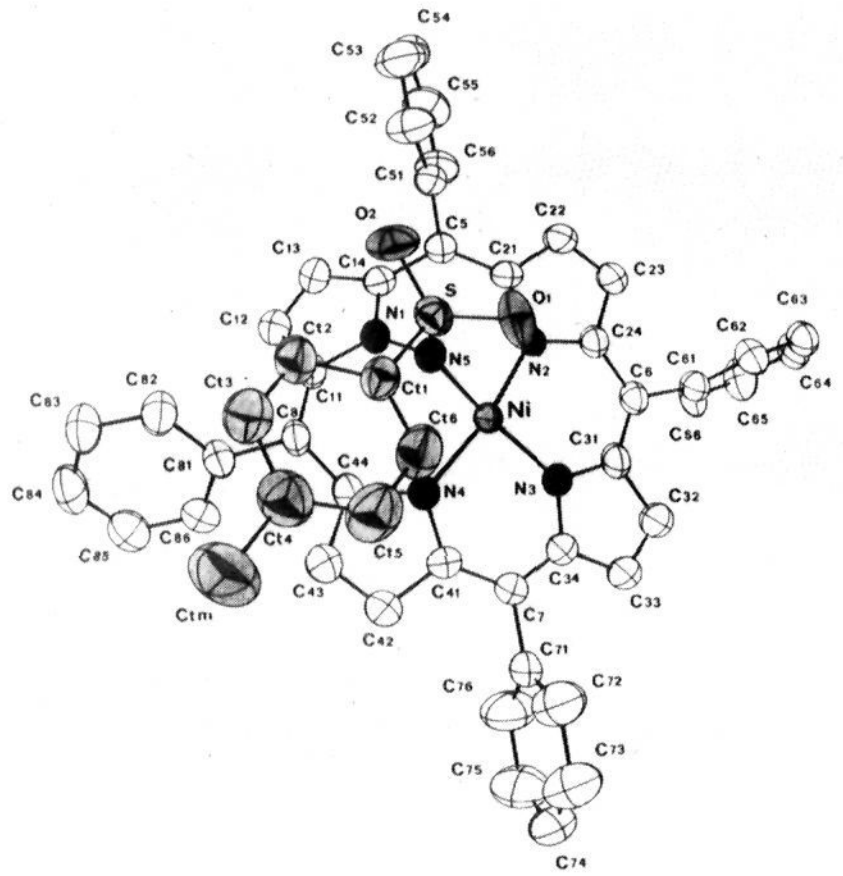

Figure 1. Computer-drawn model of the compound. The ellipsoids (50% probability) represent the thermal motions of the atoms as derived from the anisotropic thermal parameters listed in Table V. Each atom is identified with the symbol used throughout the paper. For clarity, nitrogens and tosyl group are artificially darkened.

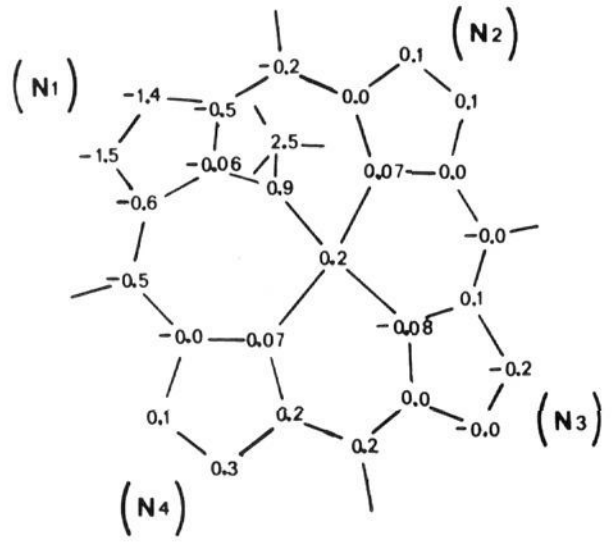

Figure 2. Diagram of the porphinato core displaying the perpendicular atomic displacements, in Å, from the mean plane of the porphinato nitrogens. The orientation of the complex is identical with that in Figure 1.

individually determined length. For comparison, the averaged bond lengths in the core of compound **19**[17] are N–Ca = 1.382 (6), C_a–C_b = 1.434 (8), C_b–C_b = 1.344 (6), C_a–C_m = 1.398 (7), and C_m–C_p = 1.496 (8) Å. These distances are quite similar to those found in normal metalloporphyrin complexes,[23] showing that a nitrene or a carbene fragment inserted into a Ni–N bond has little or no effect on π-electron delocalization in the porphinato core.

The plane defined by the Ni, Nl, N5 and the sulfur atom S is almost perpendicular to the (4N) plane (89.7°). The tosyl group is bound to N5 so that it lies above the macrocycle making a dihedral angle of 17.9° with the (4N) plane (see Table III). On the other hand, the phenyl groups are tilted with respect to the plane of the three neighboring carbons of the bridge position between pyrroles; the tilted angles of the four phenyls Ph(5)–Ph(8) are 73.0, 76.8, 86.1, and 51.9°. The average value of the internal angles in the phenyl rings is 119.96 (8)° and the average value of the C–C bond distances is 1.378 (14) Å.

Table I. Bond Lengths and Angles in the Coordination Group and in the Porphinato Skeleton

	Bond Lengths, Å		
Ni–N_2	1.920 (3)	N4–C41	1.369 (6)
Ni–N3	1.883 (4)	C41–C42	1.440 (8)
Ni–N4	1.920 (4)	C42–C43	1.332 (8)
Ni–N5	1.830 (4)	C43–C44	1.442 (7)
		C44–N4	1.407 (7)
N1–C11	1.374 (6)		
C11–C12	1.435 (6)	N5–N1	1.380 (5)
C12–C13	1.357 (7)	N5–S	1.608 (4)
C13–C14	1.419 (7)	S–O1	1.441 (4)
C14–N1	1.363 (5)	S–O2	1.429 (4)
		S-Ctl	1.769 (5)
N2–C21	1.419 (6)	Ct1–Ct2	1.403 (8)
C21–C22	1.434 (7)	Ct2–Ct3	1.356 (8)
C22–C23	1.338 (7)	Ct3–Ct4	1.400 (9)
C23–C24	1.433 (7)	Ct4–Ct5	1.382 (10)
C24–N2	1.371 (6)	Ct5–Ct6	1.384 (9)
		Ct6–Ct1	1.378 (8)
N3–C31	1.377 (7)	Ct4–Ctm	1.521 (10)
C31–C32	1.451 (8)		
C32–C33	1.334 (8)		
C33–C34	1.442 (9)		
C34–N3	1.374 (6)		
	Bond Angles, deg		
N2–Ni–N3	94.0 (1)	Ni–N5–N1	109.7 (2)
N3–Ni–N4	94.1 (1)	Ni–N5–S	132.3 (1)
N4–Ni–N5	87.3 (1)	N1–N5–S	117.9 (2)
N5–Ni–N2	87.2 (1)	N5–N1–C11	124.9 (4)
N2–Ni–N4	167.1 (2)	N5–N1–C14	121.7 (4)
N3–Ni–N5	165.6 (2)	N1–C11–C12	103.6 (4)
		C11–C12–C13	109.2 (4)
Ni–N2–C21	129.8 (2)	C12–C13–C14	108.7 (4)
Ni–N2–C24	124.7 (2)	C13–C14–N1	104.9 (4)
N2–C21–C22	108.0 (4)	C14–N1–C11	113.2 (4)
C21–C22–C23	108.9 (4)	N1–C11–C8	124.7 (4)
C22–C23–C24	106.7 (4)	C8–C11–C12	131.3 (5)
C23–C24–N2	110.9 (4)	N1–C14–C5	122.7 (4)
C24–N2–C21	105.1 (4)	C5–C14–C13	131.8 (4)
N2–C21–C5	131.2 (4)		
C5–C21–C22	119.7 (4)		
N2–C24–C6	124.7 (4)	N5–S–O1	104.5 (2)
C6–C24–C23	124.2 (4)	N5–S–O2	109.8 (2)
		O1–S–O2	120.5 (3)
Ni–N3–C31	126.2 (2)		
Ni–N3–C34	125.0 (2)		
N3–C31–C32	108.0 (4)	Ct1–S–O1	105.6 (2)
C31–C32–C33	108.0 (5)	Ct1–S–O2	107.6 (2)
C32–C33–C34	107.5 (5)	Ct1–S–N5	108.0 (2)
C33–C34–N3	108.8 (4)	S–Ct1–Ct2	120.7 (3)
C34–N3–C31	107.3 (4)	S–Ct1–Ct6	118.7 (3)
N3–C31–C6	125.5 (4)	Ct1–Ct2–Ct3	118.5 (5)
C6–C31–C32	126.0 (5)	Ct2–Ct3–Ct4	122.6 (6)
N3–C34–C7	125.0 (4)	Ct3–Ct4–Ct5	117.3 (6)
C7–C34–C33	126.0 (5)	Ct4–Ct5–Ct6	121.6 (6)
		Ct5–Ct6–Ct1	119.3 (6)
Ni–N4–C41	123.6 (2)	Ct6–Ct1–Ct2	120.5 (5)
Ni–N4–C44	130.3 (2)	Ct3–Ct4–Ctm	122.2 (6)
N4–C41–C42	110.9 (4)	Ct5–Ct4–Ctm	120.4 (7)
C41–C42–C43	105.9 (5)		
C42–C43–C44	109.7 (5)		
C43–C44–N4	107.3 (4)		
C44–N4–C41	105.7 (4)		
N4–C41–C7	124.1 (4)		
C7–C41–C42	124.5 (5)		
N4–C44–C8	130.8 (4)		
C8–C44–C43	121.3 (4)		

A stereoscopic view of the complex is shown in Figure 3. Some selected intra- and intermolecular distances are listed in Table IV.

Table II. Bond Lengths and Angles in the Peripheral Phenyl Groups and in the Dichloromethane Solvate

bond lengths, Å		bond angles, deg	
C5-C14	1.403 (7)	C14-C5-C21	126.6 (4)
C5-C21	1.402 (7)	C14-C5-C51	113.9 (4)
C5-C51	1.470 (6)	C21-C5-C51	119.3 (4)
C51-C52	1.381 (9)	C5-C51-C52	118.6 (5)
C52-C53	1.385 (9)	C5-C51-C56	122.8 (5)
C53-C54	1.349 (10)	C51-C52-C53	121.3 (6)
C54-C55	1.374 (12)	C52-C53-C54	119.1 (6)
C55-C56	1.390 (9)	C53-C54-C55	121.4 (7)
C56-C51	1.378 (7)	C54-C55-C56	119.1 (6)
		C55-C56-C51	120.5 (6)
C6-C24	1.417 (7)	C56-C51-C52	118.4 (5)
C6-C31	1.368 (7)		
C6-C61	1.496 (7)	C24-C6-C31	123.4 (4)
C61-C62	1.380 (8)	C24-C6-C61	115.5 (4)
C62-C63	1.380 (8)	C31-C6-C61	120.9 (4)
C63-C64	1.366 (8)	C6-C61-C62	120.8 (4)
C64-C65	1.385 (9)	C6-C61-C66	120.6 (5)
C65-C66	1.381 (8)	C61-C62-C63	121.8 (5)
C66-C61	1.379 (7)	C62-C63-C64	119.2 (5)
		C63-C64-C65	120.2 (5)
C7-C34	1.376 (7)	C64-C65-C66	119.7 (6)
C7-C41	1.407 (8)	C65-C66-C61	120.8 (5)
C7-C71	1.511 (7)	C66-C61-C62	118.1 (5)
C71-C72	1.362 (8)		
C72-C73	1.392 (10)	C34-C7-C41	124.3 (5)
C73-C74	1.310 (14)	C34-C7-C71	119.1 (4)
C74-C75	1.380 (12)	C41-C7-C71	116.5 (4)
C75-C76	1.416 (10)	C7-C71-C72	120.0 (5)
C76-C71	1.365 (11)	C7-C71-C76	120.5 (5)
		C71-C72-C73	120.3 (7)
C8-C11	1.379 (6)	C72-C73-C74	121.7 (8)
C8-C44	1.424 (6)	C73-C74-C75	119.4 (8)
C8-C81	1.481 (7)	C74-C75-C76	120.1 (8)
C81-C82	1.403 (8)	C75-C76-C71	118.9 (7)
C82-C83	1.398 (9)	C76-C71-C72	119.4 (6)
C83-C84	1.367 (10)		
C84-C85	1.378 (11)	C11-C8-C44	126.0 (4)
C85-C86	1.396 (9)	C11-C8-C81	114.7 (4)
C86-C81	1.376 (9)	C44-C8-C81	118.9 (4)
		C8-C81-C82	119.7 (4)
C9-Cl1	1.702 (9)	C8-C81-C86	122.2 (5)
C9-Cl2	1.734 (12)	C81-C82-C83	121.1 (5)
		C82-C83-C84	119.6 (6)
		C83-C84-C5	120.0 (6)
		C84-C85-C86	120.1 (6)
		C85-C86-C81	121.1 (5)
		C86-C81-C82	117.6 (5)
		Cl1-C9-C12	113.4 (4)

Table III. Least-Squares Planes

Planes and Deviations (Å)[a]					
plane (4N): N1,N2,N2,N4					
N1	0.065 (4)	N3	0.081 (4)	Ni	−0.2147 (8)*
N2	−0.069 (3)	N4	−0.074 (4)	N5	−0.940 (4)*
plane (N1): N1,C11-C14					
N1	−0.020 (4)	C12	−0.002 (5)	C14	0.030 (5)
C11	0.019 (5)	C13	−0.018 (5)	N5	−0.175 (4)*
plane (N2): N2,C21-C24					
N2	−0.017 (3)	C22	−0.016 (5)	C24	0.018 (4)
C21	0.024 (5)	C23	−0.002 (5)		
plane (N3): N3,C31-C34					
N3	0.012 (4)	C32	0.010 (6)	C34	−0.016 (5)
C31	−0.017 (5)	C33	0.006 (6)		
plane (N4): N4,C41-C44					
N4	−0.020 (4)	C42	−0.007 (6)	C44	0.027 (5)
C41	0.026 (5)	C43	−0.018 (6)		
plane (T): Ct1-Ct6					
Ct1	−0.004 (5)	Ct4	−0.001 (7)	S	0.028 (1)*
Ct2	0.007 (6)	Ct5	0.004 (7)	Ctm	0.008 (9)*
Ct3	−0.006 (7)	Ct6	0.001 (6)		
plane (P): Ni,N1,N5,S					
Ni	0.0000 (8)	N5	−0.0010 (43)		
N1	0.0003 (42)	S	0.0000 (15)		

Equations[b]

plane	*A*	*B*	*C*	*D*
(4N)	0.251	−0.646	−0.720	−2.393
(N1)	0.488	−0.143	−0.872	−2.330
(N2)	0.227	−0.634	−0.738	−2.422
(N3)	0.298	−0.681	−0.668	−2.292
(N4)	0.386	−0.555	−0.736	−1.914
(T)	0.523	−0.636	−0.567	−4.254
(P)	−0.801	0.274	−0.531	−1.439

Angles (deg) between Planes

(4N)-(N1)	40.5	(4N)-(T)	17.9
(4N)-(N2)	1.8		
(4N)-(N3)	4.4	(4N)-(P)	89.7
(4N)-(N4)	9.4		
(N1)-(N2)	40.1	(N1)-(T)	40.5
(N2)-(N3)	6.3	(N2)-(T)	19.6
(N3)-(N4)	9.6	(N3)-(T)	14.4
(N4)-(N1)	32.9	(N4)-(T)	13.2
(N1)-(N3)	42.3		
(N2)-(N4)	10.2		

[a] An asterisk indicates atoms not included in the calculation. [b] Equations are in the form $AX + BY + CZ = D$. *X, Y, Z* refer to the axial system *a, c** ∧ *a, c**.

Experimental Section

General. Infrared and visible spectra were recorded on a Perkin-Elmer 457 and a Cary 118 spectrophotometer, respectively. Proton magnetic resonance spectra (NMR) were recorded on a Perkin-Elmer Model R12 and a Bruker Model W H 90 at 60 or 90 MHz. The chemical shifts are expressed in δ values (ppm) relative to tetramethylsilane internal standard and the coupling constants in hertz (s, singlet; d, doublet; t, triplet; q, quadruplet; m, multiplet). Mass spectra (70 eV) were recorded on a Thomson-Houston THN 208 mass spectrometer. Combustion analyses were performed by the Service Central de Microanalyses du CNRS, Division de Strasbourg. All analyses agree with calculated values within ±0.4%, except when figures are given in full. Separation and purification of the products were obtained using Merck standardized alumina (II-III).

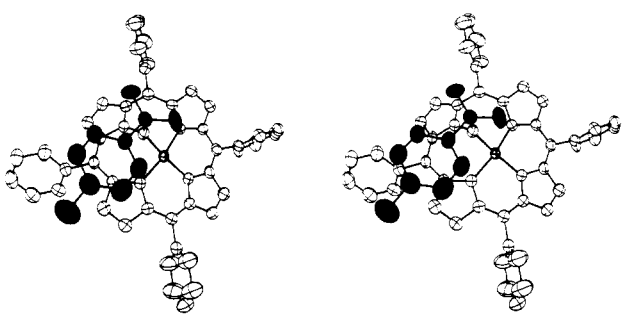

Figure 3. Stereoscopic view of the structure.

***N*-Tosylamino-5,10,15,20-tetraphenylporphin (4).** A solution of ZnTPP (0.5 g) and *p*-toluenesulfonyl azide (2.0 g) in CH_2Cl_2 (500 mL) in six stoppered 100-mL Erlenmeyer flasks was left for ca. 8 h in sunlight. At this stage no further change in the reaction mixture was apparent (TLC). To the solution was added 16 N HCl (5 mL) with vigorous shaking. After 0.5 h excess solid ammonium carbonate was added, the slurry filtered on a sintered glass, and the solution evaporated to dryness under vacuum. Chromatography of the residue (250 g of alumina, CH_2Cl_2) successively yielded H_2TPP (160 mg) and base **4** (237 mg, 63% based on transformed starting material), as violet crystals from CH_2Cl_2-CH_3OH. Base **4** showed NMR ($CDCl_3$) δ −0.05 (broad 2, NH), 2.3 (s, 3, CH_3), 4.86 (d, 2, J = 8 Hz, tolyl), 6.36 (d, 2, J = 8 Hz, tolyl), 7.6-8.5 (m, 20, phenyl), 7.85 (s,

Table IV. Interatomic Distances (Å)

Selected Intramolecular Contacts			
Ni···N1	2.639 (4)	N1···N2	3.117 (5)
		N1···N3	2.783 (5)
Ni···C5	3.626 (4)	N3···N4	2.784 (6)
Ni···C6	3.311 (5)	N4···N1	3.118 (5)
Ni···C7	3.276 (5)		
Ni···C8	3.624 (5)	N1···N3	4.483 (6)
		N2···N4	3.816 (5)
N5···N2	2.587 (5)		
N5···N4	2.590 (6)		

Intermolecular Distances Less Than 3.6 Å[a]

C12···C24	2/000	3.469 (6)	O1···C64	2/010	3.286 (8)
C12···C23	2/000	3.497 (7)	O1···C9	2/111	3.298 (11)
C13···N2	2/000	3.548 (6)	O1···C63	2/010	3.311 (7)
C13···C24	2/000	3.559 (7)	C54···C54	2/$\bar{1}$00	3.491 (9)
N4···C56	2/000	3.497 (7)			

Contacts around the Dichloromethane Solvate Less Than 3.9 Å[a]

C9···O1	2/111	3.298 (11)	Cl2···C32	2/111	3.672 (7)
C9···C63	1/101	3.751 (11)	Cl2···C31	2/111	3.702 (5)
C9···N3	2/111	3.753 (11)	Cl2···C85	2/101	3.740 (7)
C9···C31	2/111	3.870 (12)	Cl2···C23	1/101	3.789 (6)
Cl1···Ct6	2/111	3.828 (7)	Cl2···C62	2/111	3.818 (5)
Cl1···C84	2/101	3.883 (7)	Cl2···C6	2/111	3.899 (5)

[a] Second atoms not in the crystal chemical unit (i.e., not listed in Table I) are specified by the subscript *I/uvw* which denotes the manner in which the atomic parameters can be derived from the corresponding atom in the crystal unit. *I* refers to one of the following symmetry operations: 1, *xyz*; 2, $\bar{x}\bar{y}\bar{z}$. The *u*, *v*, *w* digits code a lattice translation as $ua + vb + wc$.

2, pyrrole), 8.7 (s, 2, pyrrole), 8.86 (broad, s, 4, pyrrole); visible (CH_2Cl_2) λ_{max} 432 nm (ϵ 218 000), 510 (2300), 548 (9300), 585 (10 000), 640 (7900). Anal. ($C_{51}H_{37}N_5O_2S$) C, H, N.

***N*-*p*-Nitrobenzoylamino-5,10,15,20-tetraphenylporphin (5).** Base **5** was prepared in the same way as described above for base **4** (same yield). Base **5** showed IR ν_{max} (KBr) 1615 cm^{-1} (C=O); NMR ($CDCl_3$) δ −0.6 (broad, 2, NH), 3.44 (d, 2, J = 9 Hz, *p*-nitrophenyl), 6.36 (d, 2, J = 9 Hz, *p*-nitrophenyl), 7.7–8.35 (m, 20, phenyl), 8.11 (s, 2, pyrrole), 8.89 (s, 2, pyrrole), 8.92 (d, 2, J = 4.2 Hz, pyrrole), 9.16 (d, 2, J = 4.2 Hz, pyrrole); visible (CH_2Cl_2) λ_{max} 427 nm (ϵ 186 000), 505 (3150, shoulder), 544 (11 000), 583 (10 400), 640 (7800). Anal. ($C_{51}H_{34}N_6O_3$) C, H, N.

2-Tosyl-5,10,15,20-tetraphenylporphin (6). A suspension of copper powder (0.6 g) in dimethoxymethane (50 mL) containing ZnTPP (0.6 g) and tosyl azide (3.0 g) was stirred under reflux for 24 h. After the usual workup (demetalation and chromatography) H_2TPP (235 mg) and **6** (44 mg, 11% based on transformed starting material) could be recovered and crystallized from CH_2Cl_2–CH_3OH. Base **6** showed NMR ($CDCl_3$) δ −2.65 (broad, 2, NH), 2.43 (s, 3, CH_3), 7.16 (d, 2, J = 8 Hz, tolyl), 7.50 (d, 2, J = 8 Hz, tolyl), 7.6–8.3 (m, 20, phenyl), 8.58 (d, 1, J = 5 Hz, pyrrole), 8.70 (s, 1, pyrrole), 8.76 (d, 1, J = 5 Hz, pyrrole), 8.89 (s, 4, pyrrole); visible (CH_2Cl_2) λ_{max} 425 nm (ϵ 205 000), 525 (10 800), 562 (3100), 605 (3000), 663 (5200); mass spectrum *m/e* 768 (M^+, 20%), 613 ($-SO_2C_6H_4CH_3$, 100%). Anal. ($C_{51}H_{37}N_4O_2S$) H, N. C: calcd, 79.56; found, 78.98.

Nickel Complex 7. A solution of **6** (30 mg) and Ni(acac)$_2$ (100 mg) in 1,2-dichloroethane (10 mL) was refluxed for 1 h. Filtration (alumina) and crystallization (CH_2Cl_2–CH_3OH) gave **7** as red crystals. **7** showed NMR ($CDCl_3$) δ 2.40 (s, 3, CH_3), 7.14 (d, J = 8 Hz, tolyl), 7.35 (d, J = 8 Hz, tolyl), 7,5–8.0 (m, 20, phenyl), 8.53 (s, 2, pyrrole), 8.65 (s, 2, pyrrole), 8.67 (s, 2, pyrrole), 9.03 (s, 1, pyrrole); visible (CH_2Cl_2) λ_{max} 423 nm (ϵ 226 000), 538 (14 200), 575 (8200). Anal. ($C_{51}H_{35}N_4O_2SNi$) C, H, N.

Azahomoporphyrin 9 and porphyrin 8. To a solution of H_2TPP (2 g) and *N*-*p*-nitrophenylsulfonyloxycarbamate[8] (2 g) in CH_2Cl_2 (2 L) was slowly added triethylamine (1 mL) in CH_2Cl_2 (50 mL) over 3.5 h. The resulting dark solution was evaporated to dryness and the residue chromatographed (300 g of alumina). Toluene eluted first H_2TPP (1.375 g) followed by **8** (20 mg) and **9** (86 mg; 4 and 12% yield based on transformed starting material). Both **8** and **9** were crystallized from methanol. Refluxing **9** in toluene for 1 h resulted in no appreciable change. **8** showed IR (KBr) ν_{max} 1725 cm^{-1} (C=O);

Table V. Fractional Atomic Coordinates[a]

Atom	*x*	*y*	*z*
Ni	0.177 31 (5)	0.211 68 (5)	0.158 49 (7)
N1	0.0709 (2)	0.0732 (2)	0.2449 (3)
C11	0.1161 (3)	0.0002 (3)	0.2806 (4)
C12	0.0380 (3)	−0.0879 (3)	0.2463 (5)
C13	−0.0461 (3)	−0.0647 (3)	0.1914 (4)
C14	−0.0253 (3)	0.0380 (3)	0.1850 (4)
N2	0.0527 (2)	0.2232 (2)	0.0666 (3)
C21	−0.0439 (3)	0.1793 (3)	0.0734 (4)
C22	−0.1109 (3)	0.2233 (4)	−0.0015 (4)
C23	−0.0604 (3)	0.2862 (3)	−0.0573 (4)
C24	0.0410 (3)	0.2850 (3)	−0.0164 (4)
N3	0.2498 (2)	0.2824 (2)	0.0657 (3)
C31	0.2138 (3)	0.3324 (3)	−0.0229 (4)
C32	0.2965 (4)	0.3891 (4)	−0.0581 (5)
C33	0.3788 (4)	0.3759 (4)	0.0106 (5)
C34	0.3507 (3)	0.3101 (3)	0.0906 (4)
N4	0.2873 (2)	0.1692 (2)	0.2451 (3)
C41	0.3833 (3)	0.2155 (3)	0.2548 (5)
C42	0.4490 (3)	0.1783 (4)	0.3413 (5)
C43	0.3921 (4)	0.1069 (4)	0.3793 (5)
C44	0.2905 (3)	0.0956 (3)	0.3183 (4)
N5	0.1141 (2)	0.1732 (2)	0.2714 (3)
S	0.1014 (1)	0.2331 (1)	0.3886 (1)
O1	0.1137 (3)	0.3339 (2)	0.3666 (3)
O2	0.0143 (2)	0.1834 (3)	0.4179 (3)
Ct1	0.2026 (3)	0.2336 (3)	0.5066 (4)
Ct2	0.1926 (4)	0.1702 (4)	0.5907 (5)
Ct3	0.2726 (5)	0.1727 (5)	0.6789 (5)
Ct4	0.3652 (4)	0.2343 (5)	0.6878 (5)
Ct5	0.3728 (5)	0.2950 (5)	0.6027 (6)
Ct6	0.2925 (4)	0.2953 (4)	0.5123 (5)
Ctm	0.4548 (5)	0.2351 (7)	0.7859 (7)
C5	−0.0804 (3)	0.0963 (3)	0.1222 (4)
C51	−0.1872 (3)	0.0609 (3)	0.1046 (4)
C52	−0.2268 (4)	0.0730 (5)	0.2002 (5)
C53	−0.3267 (5)	0.0397 (6)	0.1896 (7)
C54	−0.3857 (4)	−0.0071 (5)	0.0841 (7)
C55	−0.3493 (5)	−0.0208 (5)	−0.0133 (7)
C56	−0.2492 (4)	0.0130 (5)	−0.0022 (5)
C6	0.1176 (3)	0.3362 (3)	−0.0613 (4)
C61	0.0868 (3)	0.3943 (3)	−0.1573 (4)
C62	0.0604 (4)	0.4818 (3)	−0.1324 (4)
C63	0.0196 (3)	0.5298 (4)	−0.2208 (5)
C64	0.0049 (4)	0.4899 (4)	−0.3361 (5)
C65	0.0329 (5)	0.4035 (4)	−0.3638 (5)
C66	0.0741 (4)	0.3567 (4)	−0.2742 (5)
C7	0.4137 (3)	0.2818 (3)	0.1804 (5)
C71	0.5232 (5)	0.3222 (4)	0.2012 (5)
C72	0.5703 (5)	0.4041 (5)	0.2826 (7)
C73	0.6716 (5)	0.4402 (6)	0.3043 (8)
C74	0.7244 (5)	0.3978 (6)	0.2473 (8)
C75	0.6788 (5)	0.3152 (7)	0.1635 (9)
C76	0.5757 (5)	0.2773 (5)	0.1387 (8)
C8	0.2158 (3)	0.0140 (3)	0.3273 (4)
C81	0.2449 (3)	−0.0700 (3)	0.3812 (4)
C82	0.1980 (4)	−0.1102 (4)	0.4642 (5)
C83	0.2170 (4)	−0.1953 (4)	0.5083 (5)
C84	0.2848 (5)	−0.2384 (4)	0.4730 (6)
C85	0.3312 (4)	−0.2006 (4)	0.3908 (6)
C86	0.3103 (4)	−0.1171 (4)	0.3447 (5)
Solvate			
C9	0.7467 (7)	0.4914 (7)	0.732 (1)
Cl1	0.6372 (1)	0.4747 (1)	0.6307 (2)
Cl2	0.7403 (2)	0.4213 (2)	0.8450 (2)

[a] Estimated standard deviations are given in parentheses in this and all tables.

NMR ($CDCl_3$) δ −2.7 (broad s, 2, porphyrin NH), 1.35 (t, 3, J = 7 Hz, CH_3), 4.28 (q, 2, J = 7 Hz, CH_2), 7.15 (broad s, 1, NH), 7.7–8.5 (m, 20, phenyl), 8.65–8.90 (m, 6, pyrrole), 9.07 (s, 1, pyrrole); visible (CH_2Cl_2) λ_{max} 419 nm (ϵ 253 000), 515 (22 700), 548 (6200), 590

Table VI. Anisotropic Thermal Parameters[a]

Atom	U_{11}	U_{22}	U_{33}	U_{12}	U_{13}	U_{23}
Ni	0.0382 (4)	0.0420 (4)	0.0407 (4)	0.0132 (3)	0.0127 (3)	0.0168 (3)
N1	0.047 (2)	0.041 (2)	0.044 (2)	0.015 (1)	0.016 (1)	0.017 (1)
C11	0.051 (2)	0.039 (2)	0.042 (2)	0.016 (2)	0.016 (2)	0.015 (2)
C12	0.053 (3)	0.044 (3)	0.059 (3)	0.010 (2)	0.015 (2)	0.015 (2)
C13	0.055 (3)	0.044 (3)	0.058 (3)	0.010 (2)	0.019 (2)	0.017 (2)
C14	0.039 (2)	0.054 (3)	0.047 (3)	0.015 (2)	0.016 (2)	0.017 (2)
N2	0.043 (2)	0.042 (2)	0.043 (2)	0.017 (1)	0.014 (1)	0.013 (1)
C21	0.036 (2)	0.048 (2)	0.046 (2)	0.015 (2)	0.017 (2)	0.011 (2)
C22	0.039 (2)	0.062 (3)	0.053 (3)	0.019 (2)	0.013 (2)	0.020 (2)
C23	0.044 (2)	0.052 (3)	0.051 (3)	0.020 (2)	0.011 (2)	0.019 (2)
C24	0.047 (2)	0.040 (2)	0.043 (2)	0.015 (2)	0.013 (2)	0.014 (2)
N3	0.044 (2)	0.045 (2)	0.049 (2)	0.014 (1)	0.017 (2)	0.020 (2)
C31	0.057 (3)	0.051 (3)	0.055 (3)	0.024 (2)	0.023 (2)	0.027 (2)
C32	0.058 (3)	0.067 (3)	0.067 (3)	0.021 (2)	0.029 (2)	0.034 (3)
C33	0.049 (3)	0.068 (3)	0.088 (4)	0.019 (2)	0.031 (3)	0.042 (3)
C34	0.043 (2)	0.051 (3)	0.062 (3)	0.017 (2)	0.022 (2)	0.024 (2)
N4	0.042 (2)	0.047 (2)	0.048 (2)	0.014 (1)	0.013 (1)	0.018 (2)
C41	0.037 (2)	0.054 (3)	0.064 (3)	0.011 (2)	0.015 (2)	0.022 (2)
C42	0.042 (2)	0.066 (3)	0.068 (3)	0.012 (2)	0.007 (2)	0.029 (3)
C43	0.050 (3)	0.065 (3)	0.058 (3)	0.015 (2)	0.007 (2)	0.025 (3)
C44	0.046 (2)	0.049 (2)	0.043 (2)	0.017 (2)	0.010 (2)	0.017 (2)
N5	0.048 (2)	0.042 (2)	0.042 (2)	0.015 (1)	0.019 (1)	0.015 (1)
S	0.0572 (7)	0.0518 (7)	0.0488 (7)	0.0249 (6)	0.0200(6)	0.0121 (6)
O1	0.109 (3)	0.046 (2)	0.064 (2)	0.039 (2)	0.019 (2)	0.014 (2)
O2	0.055 (2)	0.096 (3)	0.061 (2)	0.022 (2)	0.034 (2)	0.014 (2)
Ct1	0.056 (3)	0.038 (2)	0.048 (3)	0.011 (2)	0.017 (2)	0.007 (2)
Ct2	0.066 (3)	0.063 (3)	0.057 (3)	0.024 (2)	0.023 (3)	0.023 (2)
Ct3	0.076 (4)	0.091 (4)	0.065 (4)	0.025 (3)	0.024 (3)	0.033 (3)
Ct4	0.077 (4)	0.085 (4)	0.063 (4)	0.031 (3)	0.019 (3)	0.017 (3)
Ct5	0.080 (4)	0.070 (4)	0.080 (4)	−0.001 (3)	0.012 (3)	0.008 (3)
Ct6	0.074 (4)	0.064 (3)	0.065 (4)	0.006 (3)	0.011 (3)	0.020 (3)
Ctm	0.081 (5)	0.151 (9)	0.091 (6)	0.044 (5)	0.006 (4)	0.038 (6)
C5	0.042 (2)	0.043 (2)	0.042 (2)	0.012 (2)	0.013 (2)	0.007 (2)
C51	0.040 (2)	0.053 (3)	0.049 (3)	0.014 (2)	0.013 (2)	0.016 (2)
C52	0.053 (3)	0.102 (5)	0.057 (3)	0.015 (3)	0.021 (3)	0.012 (3)
C53	0.058 (4)	0.136 (7)	0.087 (5)	0.030 (4)	0.031 (4)	0.044 (5)
C54	0.045 (3)	0.106 (5)	0.104 (6)	0.017 (3)	0.016 (4)	0.049 (4)
C55	0.056 (4)	0.097 (5)	0.091 (5)	0.015 (3)	−0.003 (3)	0.002 (4)
C56	0.051 (3)	0.080 (4)	0.068 (4)	0.012 (3)	0.011 (3)	0.001 (3)
C6	0.054 (2)	0.043 (2)	0.042 (2)	0.020 (2)	0.019 (2)	0.016 (2)
C61	0.048 (2)	0.053 (3)	0.048 (3)	0.021 (2)	0.020 (2)	0.023 (2)
C62	0.061 (3)	0.052 (3)	0.047 (3)	0.025 (2)	0.016 (2)	0.012 (2)
C63	0.059 (3)	0.052 (3)	0.053 (3)	0.024 (2)	0.016 (2)	0.021 (2)
C64	0.073 (3)	0.060 (3)	0.053 (3)	0.029 (3)	0.018 (2)	0.026 (2)
C65	0.106 (5)	0.064 (3)	0.043 (3)	0.032 (3)	0.024 (3)	0.015 (2)
C66	0.097 (4)	0.049 (3)	0.055 (3)	0.037 (3)	0.032 (3)	0.021 (2)
C7	0.041 (2)	0.050 (3)	0.067 (3)	0.017 (2)	0.020 (2)	0.023 (2)
C71	0.046 (3)	0.056 (3)	0.077 (4)	0.017 (3)	0.019 (3)	0.035 (3)
C72	0.063 (4)	0.083 (5)	0.121 (6)	0.007 (3)	0.028 (4)	0.015 (4)
C73	0.062 (4)	0.097 (5)	0.137 (7)	−0.001 (4)	0.026 (4)	0.020 (5)
C74	0.046 (3)	0.102 (6)	0.132 (7)	0.000 (4)	0.021 (4)	0.059 (5)
C75	0.062 (4)	0.129 (7)	0.164 (9)	0.034 (5)	0.057 (5)	0.029 (6)
C76	0.061 (4)	0.102 (5)	0.135 (7)	0.018 (4)	0.041 (4)	0.004 (5)
C8	0.052 (2)	0.039 (2)	0.046 (2)	0.020 (2)	0.018 (2)	0.018 (2)
C81	0.050 (3)	0.043 (2)	0.041 (3)	0.019 (2)	0.010 (2)	0.012 (2)
C82	0.075 (3)	0.056 (3)	0.055 (3)	0.022 (2)	0.023 (3)	0.022 (2)
C83	0.088 (4)	0.051 (3)	0.071 (4)	0.023 (3)	0.022 (3)	0.029 (3)
C84	0.088 (4)	0.051 (3)	0.080 (4)	0.029 (3)	0.012 (3)	0.028 (2)
C85	0.073 (4)	0.075 (4)	0.093 (4)	0.039 (3)	0.028 (3)	0.028 (3)
C86	0.049 (3)	0.065 (3)	0.071 (4)	0.024 (2)	0.018 (2)	0.020 (3)
C9	0.117 (7)	0.106 (7)	0.155 (9)	−0.005 (5)	0.012 (6)	0.032 (6)
Cl1	0.103 (1)	0.112 (1)	0.173 (2)	0.026 (1)	0.029 (1)	0.060 (1)
Cl2	0.157 (2)	0.134 (2)	0.129 (2)	0.045 (1)	−0.016 (1)	−0.05 (1)

[a] The form of the anisotropic thermal ellipsoid is $\exp[-2\pi^2\Sigma_i\Sigma_j a_i^* a_j^* h_i h_j U_{ij}]$.

(6900), 647 (3400). Anal. ($C_{47}H_{35}N_5O_2$) H, N. C: calcd, 80.44; found, 79.78.

9 showed IR (KBr) ν_{max} 1720 cm^{-1} (C=O); NMR ($CDCl_3$) δ 0.66 (t, 3, J = 7 Hz, CH_3), 3.62 and 3.67 (2 q, 2, J = 7 Hz, CH_2), 6.9–8.0 (m, 30, phenyl + pyrrole + NH); visible (CH_2Cl_2) λ_{max} 453 nm (ϵ 81 000), 515 (6000), 530 (4900), 600 (7100), 651 (9300), 729 (12 000). Anal. ($C_{47}H_{35}N_5O_2$) H, N. C: calcd, 80.44; found, 78.95.

Nickel Complex 10. On treatment of **9** (in CH_2Cl_2) with a slight excess of $Ni(acac)_2$, TLC showed quantitative formation of **10.** The product could only be isolated in ca. 60% yield by crystallization from methanol, the loss being due to solubility and decomposition. A green

methanol solution slowly transformed into a red solution from which no stable compound could be isolated. A half-life of ca. 0.5 h was spectroscopically determined (10^{-6} M in 1:1 CH_2Cl_2–CH_3OH). **10** showed IR (KBr) ν_{max} 1720 cm^{-1} (C=O); NMR ($CDCl_3$) δ 0.12 (t, 3, J = 7 Hz, CH_3), ca. 3.4 (m, 2, CH_2), 7.1–8.1 (m, 28, phenyl + pyrrole); visible (CH_2Cl_2) λ_{max} 451 nm (ϵ 66 000), 587 (5200), 705 (13 400). Anal. ($C_{47}H_{33}N_5O_2Ni$) C, H, N.

Nickel Complex 11. A solution of $Ni(OAc)_2 \cdot 4H_2O$ (100 mg) in warm CH_3OH (10 mL) was added to **4** (30 mg) in refluxing $CHCl_3$ (10 mL). After 0.5 h $CHCl_3$ was boiled off and the product crystallized from CH_3OH (25 mg, 78%). **11** showed NMR ($CDCl_3$) δ 2.14 (s, 3, CH_3), 5.38 (d, 2, J = 8 Hz, tolyl), 6.55 (d, 2, J = 8 Hz, tolyl), 7.31 (s, 2, pyrrole), 7.65–8.35 (m, 20, phenyl), 8.65 (d, 2, J = 4.5 Hz, pyrrole), 8.72 (d, 2, J = 4.5 Hz, pyrrole), 8.74 (s, 2, pyrrole); visible (CH_2Cl_2) λ_{max} 425 nm (ϵ 126 000), 566 (11 800), 585 (10 800, sh). Anal. ($C_{51}H_{35}N_5O_2SNi$) H, N. C: calcd, 72.78; found, 71.96.

Copper complex 12 was prepared in the same way as described for **11** using copper acetate except that $CHCl_3$ was replaced by CH_2Cl_2 and that the reaction time was ca. 0.2 h (90%). **12** showed visible (CH_2Cl_2) λ_{max} 432 nm (ϵ 177 000), 560 (9200), 593 (11 400). Anal. ($C_{51}H_{35}N_5O_2SCu$) H, N. C: calcd, 72.36; found, 70.52.

Zinc complex 13 was prepared in the same way as described for **12** (80%). **13** showed NMR ($CDCl_3$) δ 2.22 (s, 3, CH_3), 5.63 (d, 2, J = 8 Hz, tolyl), 6.73 (d, 2, J = 8 Hz, tolyl), 7.41 (s, 2, pyrrole), 7.7–8.5 (m, 20, phenyl), 8.83 (s, 2, pyrrole), 8.89 (d, 2, J = 5 Hz, pyrrole), 9.00 (d, 2, J = 5 Hz, pyrrole); visible (CH_2Cl_2) λ_{max} 433 nm (ϵ 171 000), 520 (2800, sh), 560 (6300, sh), 590 (11 100, sh), 612 (13 500). Anal. ($C_{51}H_{35}N_5O_2SZn$) C, H, N.

Nickel complex 14 and copper complex 15 were prepared in the same way as **11** and **12** starting from base **5** (90 and 93%).

14 showed IR (KBr) ν_{max} 1620 cm^{-1} (C=O); NMR ($CDCl_3$) δ 4.92 (d, 2, J = 9 Hz, p-nitrophenyl), 6.80 (d, 2, p-nitrophenyl), 7.57 (s, 2, pyrrole), 7.65–8.2 (m, 20, phenyl), 8.68 (d, 2, J = 5.3 Hz, pyrrole), 8.71 (s, 2, pyrrole), 8.98 (d, 2, J = 5.3 Hz, pyrrole); visible (CH_2Cl_2) λ_{max} 420 nm (ϵ 125 000), 560 (11 500), 585 (9000, sh). Anal. ($C_{51}H_{32}N_6O_3Ni$) C, H, N.

15 showed IR (KBr) ν_{max} 1625 cm^{-1} (C=O); visible (CH_2Cl_2) λ_{max} 429 nm (ϵ 213 000), 558 (10 800), 592 (11 600). Anal. ($C_{51}H_{32}N_6O_3Cu$) C, H, N.

Mercury complex 16 was obtained by mixing a solution of base **4** (45 mg) in CH_2Cl_2 (10 mL) and a solution of $HgCl_2$ (130 mg) in CH_3OH (10 mL) followed by addition of solid NaOAc or Na_2CO_3 (100 mg). CH_2Cl_2 was boiled off from the solution and the product crystallized as blue needles (66 mg, 92%). **16** showed NMR ($CDCl_3$) δ 2.30 (s, 3, CH_3), 6.18 (d, 2, J = 8 Hz, tolyl), 6.96 (d, 2, J = 8 Hz, tolyl), 7.62 (s, 2, pyrrole, J^{199}Hg–H = 5.8 Hz), 7.7–8.35 (m, 20, phenyl), 8.77 (d, 2, J = 4.8 Hz, pyrrole, J^{199}Hg–H = ca. 5.5 Hz), 8.89 (d, 2, J = 4.8 Hz, pyrrole, J^{199}Hg–H = ca. 6 Hz), 9.09 (s, 2, pyrrole, J^{199}Hg–H = 21 Hz); visible (CH_2Cl_2) λ_{max} 450 nm (ϵ 241 000), 520 (5800, sh), 550 (9800), 604 (15 000), 660 (7000). Anal. Calcd for $C_{51}H_{35}N_5O_2Cl_2SHg_2$: C, 48.84; H, 2.81; N, 5.59. Found: C, 48.35; H, 3.14; N, 6.18.

X-Ray Study of Compound 11. Well-formed crystals were obtained from dichloromethane–methanol solutions by standing at room temperature. Crystal data: $C_{51}H_{35}N_5O_2SNi \cdot CH_2Cl_2$; mol wt 925.59; triclinic; a = 14.378 (7), b = 14.002 (7), c = 11.750 (5) Å; α = 95.62 (8), β = 102.98 (8), γ = 102.19 (8)°; U = 2226.7 Å^3; Z = 2; F_{000} = 976; d_{calcd} = 1.380, d_{obsd} = 1.37 g cm^{-3}; space group $P\bar{1}$ (no. 2); Cu Kα (λ = 1.541 78 Å) radiation for cell dimension and intensity measurements; μ (Cu Kα) = 25.1 cm^{-1}.

Preliminary x-ray examination established a two-molecule triclinic unit cell. The $P\bar{1}$ space group was confirmed by the determination of structure. Precise lattice constants and diffracted intensities were derived from measurements carried out on a Philips PW 1100 diffractometer using a crystal of dimensions 0.16 × 0.20 × 0.32 mm. The setting angles of 25 reflections with 2θ values in the range 13–40° were determined using the automatic centering program supplied with the computer-controlled diffractometer. Least-squares refinement of these reflections led to the lattice constants reported above. The measured density reported was obtained by flotation in aqueous zinc chloride solution.

Intensity data were collected by θ–2θ scanning using graphite-monochromated Cu Kα radiation. The intensities of 6834 unique reflections were measured out to a sin θ/λ of 0.56 Å^{-1}. The scan range employed was 0.90 + 0.28 (tan θ) at a constant rate of 2.4° min^{-1}. Background was counted at both ends of the scan for 6 s. All data having $I > 3\sigma_I$ were retained as objectively observed leading to 4413 independent data used for the determination and refinement of structure. Standard deviations σ_I were calculated as previousky described[24] using a p value of 0.09. The intensities of three standard reflections were monitored throughout the data collection and measured every 90 min. None of these control reflections showed any significant changes in intensity during the course of data collection. The intensity data were reduced to a set of relative squared amplitudes, $|F_o|^2$, by application of the standard Lorentz and polarization factors. No absorption correction was applied.

The structure was solved by the heavy-atom method. The coordinates of the nickel atoms were obtained from a three-dimensional Patterson function. Using the calculated contribution of nickel to determine the phases, a Fourier synthesis revealed all nonhydrogen atoms defining the complex and the CH_2Cl_2 solvate molecule. In all structure factor calculations the atomic scattering factors used were taken from the usual sources.[25] The effect of anomalous dispersion was included for nickel, sulfur, oxygen, and chlorine atoms; the values of $\Delta f'$ and $\Delta f''$ used are those given in ref 26.

The structure was refined by full-matrix least-squares methods.[27] The quantity minimized was $\Sigma w(|F_o| - |F_c|)^2$, where the weights w were taken as $1/\sigma(F_o^2)$. All nonhydrogen atoms were refined assuming anisotropic thermal motion. The atomic parameters were grouped in several blocks due to limitations of the computer memory. The refinement of the structure converged to $R_1 = \Sigma||F_o| - |F_c||/\Sigma|F_o|$ of 0.078. Except for the C_{tm} methyl carbon, the contributions of hydrogen atoms were then introduced in calculated positions (C–H 1.00 Å). These hydrogens were assumed to have isotropic thermal motion ($B_H = B_c + 1.0$). The R_1 value was reduced to 0.070. The hydrogen atoms were then added as fixed contributions in the subsequent refinement. The final value of R_1 was 0.061, that of $R_2 = [\Sigma w(|F_o| - |F_c|)^2/\Sigma w|F_o|^2]^{1/2}$ was 0.087. The estimated standard deviation of an observation of unit weight was 1.50. A final difference synthesis had no peaks of magnitude greater than 0.6 e Å^{-3}. The final atomic positional and thermal parameters are listed in Tables V and VI, respectively.[28]

Supplementary Material Available: Listings of structure factors (12 pages). Ordering information is given on any current masthead page.

References and Notes

(1) (a) Laboratoire associé au CNRS (LA no. 31); (b) Laboratoire de Cristallochimie associé au CNRS (ERA no. 08).
(2) H. J. Callot and E. Schaeffer, *Tetrahedron*, in press. For a two-step homologation, see H. J. Callot and T. Tschamber, *J. Am. Chem. Soc.*, **97**, 6175 (1975).
(3) R. Grigg, *J. Chem. Soc. C*, 3664 (1971).
(4) K. Ichimura, *Chem. Lett.*, 641 (1976).
(5) R. Grigg, G. Shelton, A. Sweeney, and A. W. Johnson, *J. Chem. Soc., Perkin Trans. 1*, 1789 (1972); A. H. Jackson and G. R. Dearden, *Ann. N.Y. Acad. Sci.*, **206**, 151 (1973); G. M. McLaughlin, *J. Chem. Soc., Perkin Trans. 2*, 136 (1974); H. M. G. Al-Hazimi, A. H. Jackson, A. W. Johnson, and M. Winter, *J. Chem. Soc., Perkin Trans. 1*, 98 (1977).
(6) We thank Dr. A. Louati and Professor M. Gross (Université Louis Pasteur, Strasbourg) for the measurement of these data.
(7) For the effect of pyrrolic electron-withdrawing substituents on the polarographic behavior of porphyrins, see H. J. Callot, A. Giraudeau, and M. Gross, *J. Chem. Soc., Perkin Trans. 2*, 1321 (1975); A. Giraudeau, I. Ezahr, M. Gross, H. J. Callot, and J. Jordan, *Bioelectrochem. Bioenerg.*, **3**, 519 (1976).
(8) W. Lwowski and T. J. Maricich, *J. Am. Chem. Soc.*, **87**, 3630 (1965).
(9) M. F. Hudson and K. M. Smith, *Tetrahedron Lett.*, 2223 (1974).
(10) F. R. Hopf and D. G. Whitten in "Porphyrins and Metalloporphyrins", K. M. Smith, Ed., Elsevier, Amsterdam, 1975, p 675.
(11) We did not try to identify the minor components of the reaction mixture. Ring-opened oxidation products of ZnTPP have been described: B. Evans and K. M. Smith, *Tetrahedron Lett.*, 4863 (1976).
(12) See, for example, W. Lwowski and R. L. Johnson, *Tetrahedron Lett.*, 891 (1967); R. A. Abramovitch and V. Uma, *Chem. Commun.*, 797 (1968); R. A. Abramovitch, C. I. Azogu, and I. T. McMaster, *J. Am. Chem. Soc.*, **91**, 1219 (1969); R. A. Abramovitch and T. Takaya, *J. Org. Chem.*, **37**, 2022 (1972).
(13) According to the literature, the major effect of copper catalysis is an improvement of rate and yields: H. Kwart and A. A. Khan, *J. Am. Chem. Soc.*, **89**, 1950, 1951 (1967); J. I. G. Cadogan and I. Gosney, *J. Chem. Soc., Perkin Trans. 1*, 460, 466 (1974). Arylation via radical reaction and loss of SO_2 was suggested: D. S. Breslow, M. F. Sloan, N. R. Newburg, and W. Renfrew, *J. Am. Chem. Soc.*, **91**, 2273 (1969).
(14) H. J. Callot, *Bull. Soc. Chim. Fr.*, 4387 (1972); H. J. Callot and T. Tschamber, *ibid.*, 3192 (1973); H. J. Callot, A. W. Johnson, and A. Sweeney, *J. Chem. Soc., Perkin Trans. 1*, 1424 (1973).
(15) (a) B. Shah, B. Shears, and P. Hambright, *Inorg. Chem.*, **10**, 1828 (1971); D. K. Lavallee and A. E. Gebala, *ibid.*, **13**, 2004 (1974); (b) D. E. Goldberg

and K. M. Thomas, *J. Am. Chem. Soc.*, **98**, 913 (1976); O. P. Anderson and D. K. Lavallee, *ibid.*, **99**, 1404 (1977); *Inorg. Chem.*, **16**, 1634 (1977).
(16) H. J. Callot, T. Tschamber, B. Chevrier, and R. Weiss, *Angew. Chem.*, **87**, 545 (1975).
(17) B. Chevrier and R. Weiss, *J. Am. Chem. Soc.*, **98**, 2985 (1976).
(18) M. F. Hudson and K. M. Smith, *Tetrahedron Lett.*, 2227 (1974); *Tetrahedron*, **31**, 3077 (1975).
(19) R. N. Butler and A. B. Hanahoe, *J. Chem. Soc., Chem. Commun.*, 622 (1977).
(20) C. K. Johnson, Program ORTEP, ORNL 3794, 1965.
(21) L. Sacconi, *Transition Met. Chem.*, **4**, 199 (1968).
(22) V. Schomaker, J. Waser, R. E. Marsh, and G. Bergman, *Acta Crystallogr.*, **12**, 600 (1959).
(23) J. L. Hoard, *Science*, **174**, 1295 (1971); *Ann. N.Y. Acad. Sci.*, **206**, 18 (1973).
(24) B. Chevrier and R. Weiss, *J. Am. Chem. Soc.*, **97**, 1416 (1975).
(25) D. T. Cromer and J. T. Waber, *Acta Crystallogr.*, **18**, 104 (1965).
(26) "International Tables for X-Ray Crystallography", Vol. III, Kynoch Press, Birmingham, England, 1962, p 214.
(27) C. T. Prewitt, "A Fortran IV Full-Matrix Crystallographic Least-Squares Program", SFLS 5, 1966.
(28) See paragraph at end of paper regarding supplementary material.

X-Ray Photoelectron Spectroscopy of Porphyrins

J. P. Macquet, M. M. Millard, and T. Theophanides*

Contribution from the Department of Chemistry, University of Montreal, C.P. 6210, Succ. A, Montreal, Quebec H3C 3VI, Canada. *Received January 16, 1978*

Abstract: The nitrogen 1s binding energies of a series of porphyrins and several platinohematoporphyrin complexes obtained by x-ray photoelectron spectroscopy (XPS) are presented and discussed. The influence of different substituents at the periphery of the porphyrins has been studied; however, no significant change could be detected between the N_{1s} binding energies of the porphyrins studied. A value of 2 eV has been found between aza and pyrrole type nitrogen binding energies. The nature of the sitting-atop (SAT) complex reported in the literature is discussed. XPS gives strong evidence for the existence of the SAT complex, *cis*-$PtCl_2H_2$(Hemato-IX). Two types of nitrogens located at 399.9 eV for N–H and at 398.6 eV for N→Pt have been found in the SAT complex. Furthermore, the N_{1s} region for the platinohematoporphyrin Pt(Hemato-IX) shows that the four nitrogens are equivalent. A value of 399.4 eV is found for the N_{1s} binding energy of N–Pt where platinum is covalently bound to hematoporphyrin. The difference between the two types of nitrogen binding energies tends to zero in the series, H_2(Hemato-IX) (ΔE = 2.3 eV) → *cis*-$PtCl_2H_2$(Hemato-IX) (ΔE = 1.3 eV) → Pt(Hemato-IX) (ΔE = 0 eV), indicating a tendency toward equivalency upon platinum insertion.

Introduction

X-Ray photoelectron spectroscopy proved to be a useful tool for the differentiation of nitrogen atoms in porphyrins.[1-4] Two types of nitrogens are found in porphyrin free bases, the aza type, whose N_{1s} binding energy is near 398 eV, and the pyrrole type of 400 eV. On metal complexation the four nitrogen atoms become equivalent with an N_{1s} energy at 399 eV.

A very interesting problem concerning the chemistry of metalloporphyrins is the knowledge of the incorporation process of the metal inside the four nitrogen atoms of the porphyrin. This field was recently reviewed by Hambright.[5] It is now generally admitted that a certain type of interaction takes place between the porphyrin and the metal before its insertion in the porphyrin plane. The intermediate compounds called "sitting-atop" complexes were studied either in solution[6,7] or in the solid state.[8-11] A controversy is still existing for the SAT evidence in solution[12] since in some cases the green coloration generally attributed to the SAT was in fact due to the mono- and diacid forms of the porphyrin.[6] The mono-, di-, and trimetallic porphyrins with unusual geometries were described by Tsutsui and Taylor.[13]

The problem of the SAT configuration is not yet completely understood. This study provides evidence for the existence of a SAT complex, *cis*-$PtCl_2H_2$(Hemato-IX), obtained during the preparation of the platinohematoporphyrin, Pt(Hemato-IX). The influence of the two kinds of platinum fixation on the nitrogen atoms is clearly demonstrated with N_{1s} binding energies in a series of compounds.

Experimental Section

Hematoporphyrin IX, H_2(Hemato-IX), was bought from Nutritional Biochemicals Co. The platinum porphyrin complexes were prepared following the method of Macquet and Theophanides.[8] The different porphyrins used in the present study were purchased from Calbiochem, California [(H_2(Copro-I-TME), H_2(Copro-III-TME)], Man-Win, Washington, D.C. [(H_2(TPyP), H_2(Deut-IX-DME), H_2(TPP)], and Sigma, Missouri [H_2(Proton-IX-DME)]. $K_2[PtCl_4]$ from Johnson Matthey and Mallory Ltd. was recrystallised twice before use.

X-Ray photoelectron spectra were recorded on a standard 650 Du Pont spectrometer with Mg Kα x-ray target. The reference line was the carbon line at 285 eV. The compounds were run as films evaporated from chloroform solution on SiO_2 ($\frac{1}{4}$-in. disk). Under the experimental conditions employed in the present study, the full widths at half maximum (fwhm) of nitrogen peaks have been found to be 2.0 ± 0.1 eV. The accuracy of the binding energies was ±0.2 eV and no significant instrument drift was detected. The nitrogen spectra were curve fitted by a least-squares computed program using a Lorentzian function with a fwhm of 2.0 eV.

It must be noted that the two diacid species, $[H_4(\text{Hemato-IX})]^{2+}(Cl^-)_2$ and $[H_4(\text{Hemato-IX})]^{2+}[PtCl_4]^{2-}$, studied by Raman spectrophotometry[14] were found to be unstable toward x-ray irradiation. This may be due to partial denaturation under vacuum or to radiation damage.

Results

The different hematoporphyrin compounds used in the present study are given in Figure 1. For this series, binding energies of nitrogen, platinum, and chlorine atoms are reported in Table I. The N_{1s} spectrum of the starting porphyrin, H_2(Hemato-IX), is shown in Figure 2 and a comparison between the different nitrogen 1s binding energies in this series is presented in Figures 3 and 4. The binding energies were all determined from a visual inspection of the spectra with an accuracy of ±0.2 eV. In order to study the substituent effect at the periphery of the porphyrin on the N_{1s} binding energies, a series of porphyrins was considered. Their structural representation and the different N_{1s} binding energies are found in Figure 5 and in Table II. Deconvolution spectra of porphyrins

0002-7863/78/1500-4741$01.00/0